

Characteristic of novel composition $\text{Na}_x[\text{Ni}_{0.6}\text{Co}_{0.2}\text{Mn}_{0.2}]\text{O}_2$ as Cathode Materials for Sodium Ion-Batteries

Byeong-Chan Jang, Ji-Woong Shin, Jin-Joo Bae, and Jong-Tae Son*

Department of Nano-Polymer Science & Engineering,
Korea National University of Transportation Chungju, Chungbuk 380-702, Republic of Korea

Received: October 20, 2016, Accepted: January 31, 2017, Available online: April 22, 2017

Abstract: In this work, novel composition of $\text{Na}_x[\text{Ni}_{0.6}\text{Co}_{0.2}\text{Mn}_{0.2}]\text{O}_2$ ($x = 0.5$ and 1.0) layered cathode materials were synthesized by using hydroxide co-precipitation and calcined at 850, 900 and 950 °C. We studied the effects of different sodium contents and calcination temperature on the structural and electrochemical properties of this novel cathode material. The change of calcination temperature and sodium content led to different P_2 -type, P_2/P_3 -type, P_2/O_3 -type, or O_3 -type structures. The results indicate better electrochemical performance of the P_2 -type cathode materials in terms of high discharge capacity and good cycling performance, when compared to P_2/P_3 , P_2/O_3 , and O_3 -type cathode materials. $\text{Na}_{0.5}[\text{Ni}_{0.6}\text{Co}_{0.2}\text{Mn}_{0.2}]\text{O}_2$ electrode calcined at 900 °C exhibited a good capacity of 107.15 mAhg^{-1} and capacity retention over 73 % after 20 cycle. Characterization of this material will help to develop cathode materials for the Na-ion battery cathode.

Keywords: Sodium ion battery; Cathode material; Co-precipitation;

1. INTRODUCTION

Lithium ion batteries (LIBs) are being widely applied in portable electronic devices and hybrid electric vehicle (HEVs) because of their high energy density and power densities [1]. However, problems have occurred because lithium is a limited resource and has a high cost due to the rapid rise in the price [2, 3]. Rechargeable sodium-ion batteries (SIBs) have recently attracted renewed interest as an appealing alternative to LIBs for electric energy storage applications, because of their low cost and the wide availability of sodium [4]. Also, SIBs are based on the same working principle as LIBs but use sodium as the electroactive species [5-10]. Among the Na-based cathodes reported to date, layered transition-metal oxides (NaMO_2 , M = transition-metal) have attracted particular attention. For instance, compounds such as Na_xCoO_2 and Na_xNiO_2 form a layered structure [11, 12]. These compounds were shown to reversibly insert Na ions, however had limited capacity and rate capability. To overcome these issues, efforts have been focused toward developing improved electrode materials for sodium ion batteries such as $\text{NaNi}_{1/3}\text{Mn}_{1/3}\text{Co}_{1/3}\text{O}_2$ [13]. The performance of this material was explained by the presence of nickel,

manganese, and cobalt in the transition metal layer [14]. Nevertheless, the introduction of expensive cobalt increases the fabrication cost and toxicity. Hence, we design novel Ni-rich $\text{Na}[\text{Ni}_{0.6}\text{Co}_{0.2}\text{Mn}_{0.2}]\text{O}_2$ which is attractive due to the reversible capacities. Novel cathode material that is of lower cost and less toxicity would allow wider applications for the sodium intercalation battery. Recently, our group reported the electrochemical property of $\text{Na}_x[\text{Ni}_{0.6}\text{Co}_{0.2}\text{Mn}_{0.2}]\text{O}_2$ ($x = 0.6, 0.7, 0.8, 0.9, 1.0$) layered cathode materials were synthesized by the hydroxide co-precipitation method which was calcined at 900 °C for 24 h [3]. However, detailed studies on how to link synthesis temperature and sodium content are still unknown. Consequently, in this study we to interconnect the influence of synthesis temperature and sodium contents with the structural and electrochemical properties of different $\text{Na}_x[\text{Ni}_{0.6}\text{Co}_{0.2}\text{Mn}_{0.2}]\text{O}_2$ ($x = 0.5$ and 1.0) materials calcined at 850-950 °C.

2. EXPERIMENTAL

The spherical hydroxide precursor $(\text{Ni}_{0.6}\text{Co}_{0.2}\text{Mn}_{0.2})(\text{OH})_2$ was prepared by using hydroxide co-precipitation method. An aqueous solution of $\text{NiSO}_4 \cdot 6\text{H}_2\text{O}$, $\text{CoSO}_4 \cdot 7\text{H}_2\text{O}$ and $\text{MnSO}_4 \cdot \text{H}_2\text{O}$ (cationic ratio of Ni:Co:Mn = 0.6:0.2:0.2) with a concentration of 1M were pumped into a continuously stirred tank reactor (CSTR) under N_2

*To whom correspondence should be addressed: Email: jt1234@ut.ac.kr

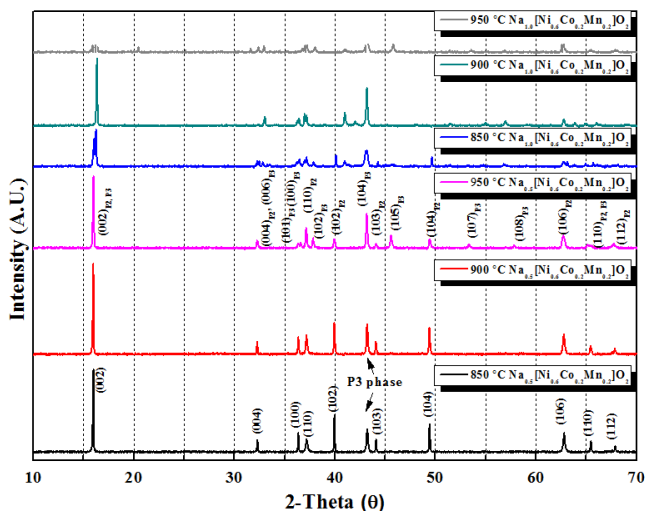


Figure 1. X-ray diffraction pattern of $\text{Na}_x[\text{Ni}_{0.6}\text{Co}_{0.2}\text{Mn}_{0.2}]\text{O}_2$ materials with different sodium contents ($x = 0.5$ and 1.0) and annealing temperature (850, 900, and 950 °C).

atmosphere. At the same time, 2 M of a NaOH solution (aq.) and the desired amount of a NH_4OH solution (aq.) as a chelating agent were also separately pumped into the reactor. The CSTR was maintained at the desired constant temperature with an appropriate stirring speed. The resulting $(\text{Ni}_{0.6}\text{Co}_{0.2}\text{Mn}_{0.2})(\text{OH})_2$ particles were filtered, washed, and then dried in a vacuum oven at 150 °C for 24 hours. The $\text{Na}_x[\text{Ni}_{0.6}\text{Co}_{0.2}\text{Mn}_{0.2}]\text{O}_2$ ($x = 0.5$ and 1.0) samples calcined of the precursor $(\text{Ni}_{0.6}\text{Co}_{0.2}\text{Mn}_{0.2})(\text{OH})_2$ and Na_2CO_3 at 850, 900, and 950 °C for 23 h in air respectively. X-ray diffraction (XRD) patterns for the cathodes were obtained using a Siemens D-5000 diffractometer in the 2θ range from 10 to 70° with $\text{CuK}\alpha$ radiation ($\lambda = 1.5406 \text{ \AA}$). The morphology of the obtained powder was observed with scanning electron microscopy (SEM). The cathode was fabricated by blending the active material, super-P carbon and binder (8 : 1 : 1) in N-methyl-2-pyrrolidone. After two hours of grinding, the viscous slurry was coated on aluminum foil using a doctor blade to make a film with uniform thickness. The film was

Table 1. The lattice parameters for $\text{Na}_x[\text{Ni}_{0.6}\text{Co}_{0.2}\text{Mn}_{0.2}]\text{O}_2$ materials with different sodium contents ($x = 0.5$ and 1.0) and annealing temperatures (850, 900, and 950 °C).

Sample	Lattice parameter		Cell volume (Å ³)
	a(Å)	c(Å)	
$\text{Na}_{0.5}[\text{Ni}_{0.6}\text{Co}_{0.2}\text{Mn}_{0.2}]\text{O}_2(850^\circ\text{C})$	2.8500 (±0.0001)	11.0772 (±0.0005)	77.9178
$\text{Na}_{0.5}[\text{Ni}_{0.6}\text{Co}_{0.2}\text{Mn}_{0.2}]\text{O}_2(900^\circ\text{C})$	2.8495 (±0.0001)	11.0790 (±0.0009)	77.9028
$\text{Na}_{0.5}[\text{Ni}_{0.6}\text{Co}_{0.2}\text{Mn}_{0.2}]\text{O}_2(950^\circ\text{C})$	2.8642 (±0.0004)	16.6509 (±0.0025)	118.29
$\text{Na}_{1.0}[\text{Ni}_{0.6}\text{Co}_{0.2}\text{Mn}_{0.2}]\text{O}_2(850^\circ\text{C})$	2.8531 (±0.0059)	16.7259 (±0.0805)	117.91
$\text{Na}_{1.0}[\text{Ni}_{0.6}\text{Co}_{0.2}\text{Mn}_{0.2}]\text{O}_2(900^\circ\text{C})$	2.9408 (±0.0046)	16.9600 (±0.0710)	127.02
$\text{Na}_{1.0}[\text{Ni}_{0.6}\text{Co}_{0.2}\text{Mn}_{0.2}]\text{O}_2(950^\circ\text{C})$	2.8808 (±0.0055)	17.3136 (±0.0381)	124.44

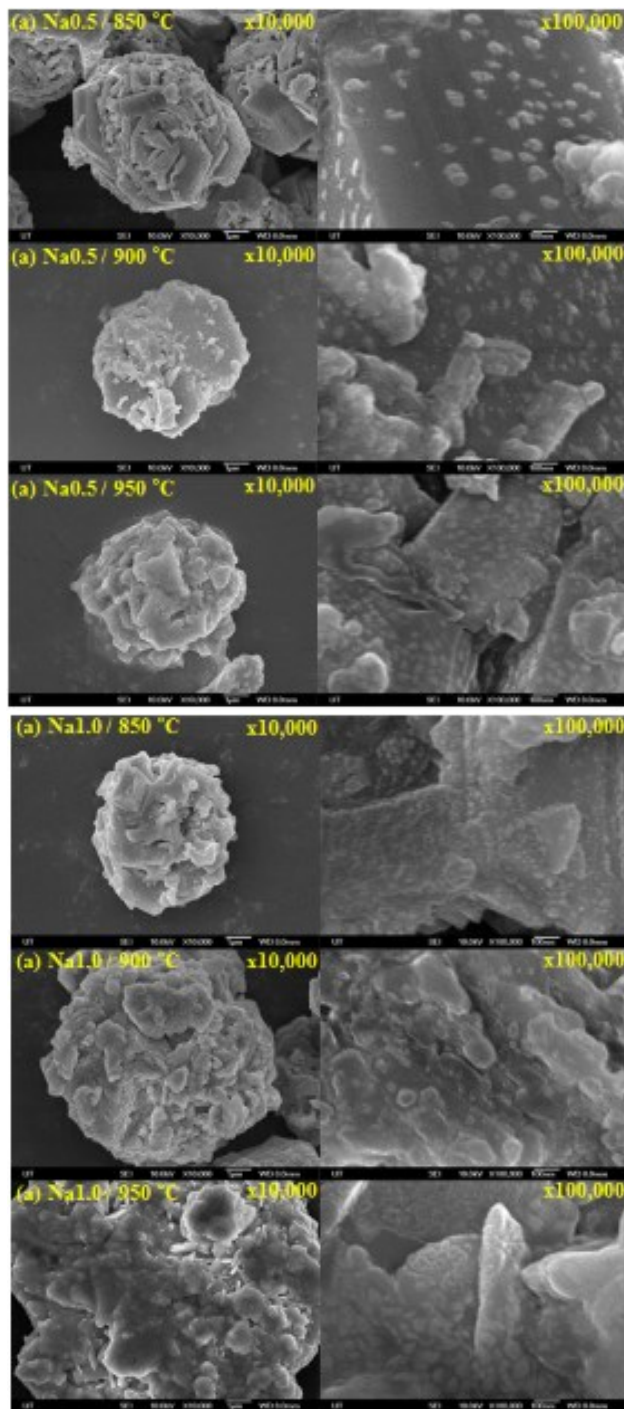


Figure 2. SEM image of $\text{Na}_x[\text{Ni}_{0.6}\text{Co}_{0.2}\text{Mn}_{0.2}]\text{O}_2$ materials with different sodium contents ($x = 0.5$ and 1.0) and annealing temperatures (850, 900, and 950 °C).

then dried at 60 °C for 6 h and 120 °C for 6 h in a vacuum oven. The electrochemical performance was measured using a CR2032 coin-type cell. Sodium-metal foil was used as the anode. Whatman glass fiber membrane and 1 M NaClO_4 electrolyte solution dissolved in a propylene carbonate(PC) were used as separator and

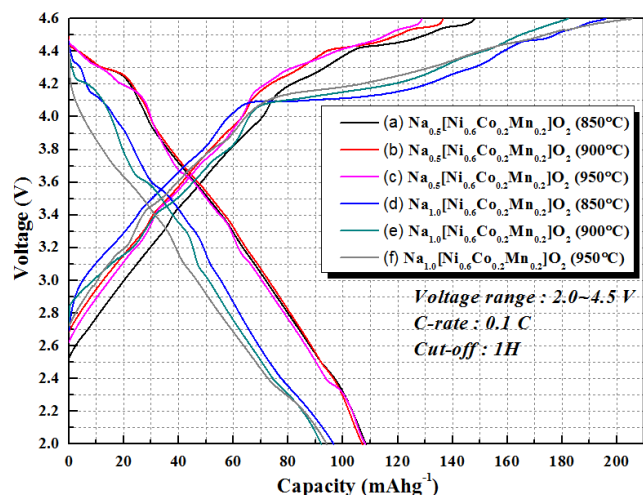


Figure 3. The initial charge and discharge curve of $\text{Na}_x[\text{Ni}_{0.6}\text{Co}_{0.2}\text{Mn}_{0.2}]\text{O}_2$ materials with different sodium contents ($x = 0.5$ and 1.0) and annealing temperatures (850 , 900 , and 950 °C) with $2.0\sim 4.6$ V at 0.1 C.

electrolyte, respectively. The cells were assembled in an argon-filled glove box. Electrochemical tests were performed at voltages between 2.0 and 4.6 V.

3. RESULTS AND DISCUSSION

Fig. 1 show XRD pattern of the $\text{Na}_x[\text{Ni}_{0.6}\text{Co}_{0.2}\text{Mn}_{0.2}]\text{O}_2$ ($x = 0.5$ and 1.0) materials with different sodium contents and calcination temperatures. The calculated lattice parameters are summarized in table 1. $\text{Na}_{0.5}[\text{Ni}_{0.6}\text{Co}_{0.2}\text{Mn}_{0.2}]\text{O}_2$ annealed at 850 and 900 °C had P_2 -type structure. $\text{Na}_{0.5}[\text{Ni}_{0.6}\text{Co}_{0.2}\text{Mn}_{0.2}]\text{O}_2$ annealed at 950 °C, had P_2 -type and P_3 -type structures. For both phases an overlapping of the (001) reflections can be observed. On the other hand, $\text{Na}_{1.0}[\text{Ni}_{0.6}\text{Co}_{0.2}\text{Mn}_{0.2}]\text{O}_2$ annealed was not formed properly at 850 - 950 °C. The SEM images of $\text{Na}_x[\text{Ni}_{0.6}\text{Co}_{0.2}\text{Mn}_{0.2}]\text{O}_2$ ($x = 0.5$ and 1.0) samples, annealed at different temperatures and sodium con-

Table. 2. The initial charge and discharge curves for $\text{Na}_x[\text{Ni}_{0.6}\text{Co}_{0.2}\text{Mn}_{0.2}]\text{O}_2$ materials with different sodium contents ($x = 0.5$ and 1.0) and annealing temperatures (850 , 900 , and 950 °C).

Sample	Charge (mAhg^{-1})	Discharge (mAhg^{-1})	effect
$\text{Na}_{0.5}[\text{Ni}_{0.6}\text{Co}_{0.2}\text{Mn}_{0.2}]\text{O}_2(850^\circ\text{C})$	148.21	108.42	73.15%
$\text{Na}_{0.5}[\text{Ni}_{0.6}\text{Co}_{0.2}\text{Mn}_{0.2}]\text{O}_2(900^\circ\text{C})$	136.57	107.15	78.56%
$\text{Na}_{0.5}[\text{Ni}_{0.6}\text{Co}_{0.2}\text{Mn}_{0.2}]\text{O}_2(950^\circ\text{C})$	128.82	108.21	84.00%
$\text{Na}_{1.0}[\text{Ni}_{0.6}\text{Co}_{0.2}\text{Mn}_{0.2}]\text{O}_2(850^\circ\text{C})$	195.90	96.65	49.34%
$\text{Na}_{1.0}[\text{Ni}_{0.6}\text{Co}_{0.2}\text{Mn}_{0.2}]\text{O}_2(900^\circ\text{C})$	182.21	92.10	50.55%
$\text{Na}_{1.0}[\text{Ni}_{0.6}\text{Co}_{0.2}\text{Mn}_{0.2}]\text{O}_2(950^\circ\text{C})$	205.51	94.10	45.79%

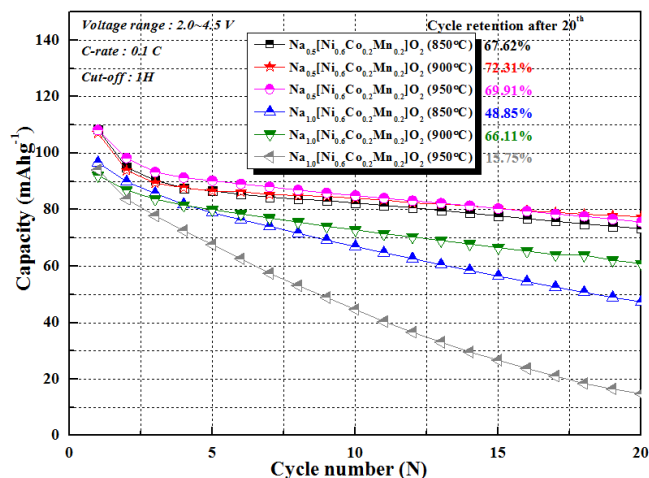


Figure 4. Cycle performance of $\text{Na}_x[\text{Ni}_{0.6}\text{Co}_{0.2}\text{Mn}_{0.2}]\text{O}_2$ materials with different sodium contents ($x = 0.5$, 1.0) and annealing temperatures (850 , 900 , and 950 °C) with 0.1 C (after 20 cycles).

tent, are shown in fig. 2. At first glance, the annealing temperature clearly has a strong influence on the particle size. There is evident distinction in particle size for the materials prepared by different sodium contents of each temperature. $\text{Na}_{0.5}[\text{Ni}_{0.6}\text{Co}_{0.2}\text{Mn}_{0.2}]\text{O}_2$ (Fig. 2 (a)-(c)) have an average particle size of about $6\sim 9$ μm and a quite homogeneous particle size distribution. Whereas, $\text{Na}_{1.0}[\text{Ni}_{0.6}\text{Co}_{0.2}\text{Mn}_{0.2}]\text{O}_2$ (Fig. 2 (e)-(f)) showed increased particle size with increasing temperature. These results demonstrate the importance of the annealing temperature as a parameter to tune the morphology and particle size, increasing the temperature increases the particle size. Also, increase in sodium contents shows that there are many impurities as well as aggregation of particles. Fig. 3 shows the initial charge and discharge curves for the $\text{Na}_x[\text{Ni}_{0.6}\text{Co}_{0.2}\text{Mn}_{0.2}]\text{O}_2$ ($x = 0.5$ and 1.0) cells in the cut-off voltage $2.0\sim 4.6$ V at 0.1 C (17mAhg^{-1}). $\text{Na}_{0.5}[\text{Ni}_{0.6}\text{Co}_{0.2}\text{Mn}_{0.2}]\text{O}_2$, annealed at 850 °C, 900 °C, and 950 °C delivered an initial discharge capacity of 108.42 , 107.15 , and 108.21 , respectively. $\text{Na}_{1.0}[\text{Ni}_{0.6}\text{Co}_{0.2}\text{Mn}_{0.2}]\text{O}_2$ annealed at 850 °C, 900 °C and 950 °C delivered an initial discharge capacity of 96.95 , 92.10 , and 94.10 mAhg^{-1} , respectively. The $\text{Na}_{0.5}[\text{Ni}_{0.6}\text{Co}_{0.2}\text{Mn}_{0.2}]\text{O}_2$ electrode delivered the higher initial discharge capacity than $\text{Na}_{1.0}[\text{Ni}_{0.6}\text{Co}_{0.2}\text{Mn}_{0.2}]\text{O}_2$. As the sodium content increased, the discharge capacity decreased. Details of the charge and discharge capacity and coulombic efficiency are summarized in Table 2. Fig. 4 shows the cycle performance of $\text{Na}_x[\text{Ni}_{0.6}\text{Co}_{0.2}\text{Mn}_{0.2}]\text{O}_2$ ($x = 0.5$ and 1.0) cells at a current density of 0.1 C (17 mAhg^{-1}) between 2.0 and 4.6 V. After 20 cycles, $\text{Na}_{0.5}[\text{Ni}_{0.6}\text{Co}_{0.2}\text{Mn}_{0.2}]\text{O}_2$ (900 °C) sample offers better cycle life and improved energy efficiency [15]. Details of the cycling efficiency is summarized in Table 3. Fig. 5 shows in the experimental synthesis phase diagram. The P_2 phase clearly forms at low temperature and sodium content. The P_2/P_3 phase clearly forms at high temperature and low sodium content. O_3/P_2 phase formed at low temperature and high sodium content. Finally, O_3 phase formed at high temperature and sodium content. Finally, the cycle characteristics were good and, the electrochemical perfor-

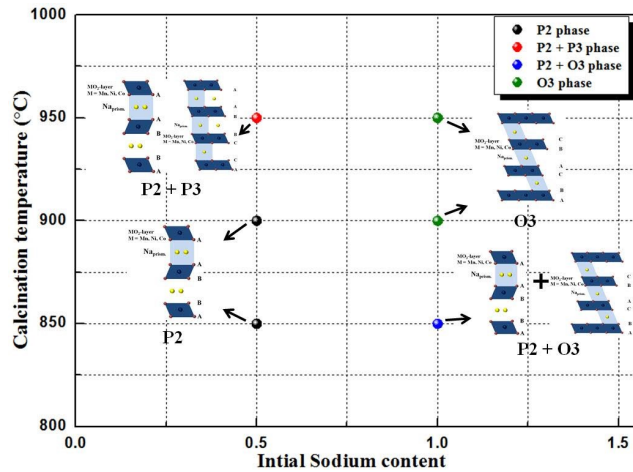


Figure 5. Synthesis phase diagram of $\text{Na}_x[\text{Ni}_{0.6}\text{Co}_{0.2}\text{Mn}_{0.2}]\text{O}_2$ ($x = 0.5$ and 1.0) for 850, 900, and 950 °C, respectively.

mance was good in the $\text{Na}_{0.5}[\text{Ni}_{0.6}\text{Co}_{0.2}\text{Mn}_{0.2}]\text{O}_2$ (900 °C) sample.

4. CONCLUSIONS

In this work, we synthesized $\text{Na}_x[\text{Ni}_{0.6}\text{Co}_{0.2}\text{Mn}_{0.2}]\text{O}_2$ layered cathode materials by hydroxide co-precipitation method. The precursor particles size ranged from 6 to 9 μm . XRD revealed the materials to have either a P2-type ($x0.5 / 850$ and 950 °C), P2/P3-type ($x0.5 / 950$ °C), P2/O3($x1.0 / 850$ °C), and O3 ($x1.0 / 900$ and 950 °C) structure. SEM image showed that an increase in sodium contents produced aggregation of particles with many impurities. The $\text{Na}_{0.5}[\text{Ni}_{0.6}\text{Co}_{0.2}\text{Mn}_{0.2}]\text{O}_2$ (900 °C) electrode exhibited a good capacity of 107.15 mAhg^{-1} and capacity retention over 73 % after 20 cycles.

5. ACKNOWLEDGMENTS

This research was supported by the Global Excellent Technology Innovation of the Korea Institute of Energy Technology Evaluation and Planning (KETEP), granted financial resource from the Ministry of Trade, Industry & Energy, Republic of Ko-

Table. 3. Cycle performance for $\text{Na}_x[\text{Ni}_{0.6}\text{Co}_{0.2}\text{Mn}_{0.2}]\text{O}_2$ materials with different sodium contents ($x = 0.5$ and 1.0) and annealing temperatures (850, 900, and 950 °C) initially and after 20 cycles.

Sample	1 st capacity (mAhg^{-1})	20 th capacity (mAhg^{-1})	Effect
$\text{Na}_{0.5}[\text{Ni}_{0.6}\text{Co}_{0.2}\text{Mn}_{0.2}]\text{O}_2(850^\circ\text{C})$	108.42	73.31	67.62 %
$\text{Na}_{0.5}[\text{Ni}_{0.6}\text{Co}_{0.2}\text{Mn}_{0.2}]\text{O}_2(900^\circ\text{C})$	107.15	77.48	72.31 %
$\text{Na}_{0.5}[\text{Ni}_{0.6}\text{Co}_{0.2}\text{Mn}_{0.2}]\text{O}_2(950^\circ\text{C})$	108.21	75.65	69.91 %
$\text{Na}_{1.0}[\text{Ni}_{0.6}\text{Co}_{0.2}\text{Mn}_{0.2}]\text{O}_2(850^\circ\text{C})$	96.95	47.36	48.85 %
$\text{Na}_{1.0}[\text{Ni}_{0.6}\text{Co}_{0.2}\text{Mn}_{0.2}]\text{O}_2(900^\circ\text{C})$	92.10	60.89	66.11 %
$\text{Na}_{1.0}[\text{Ni}_{0.6}\text{Co}_{0.2}\text{Mn}_{0.2}]\text{O}_2(950^\circ\text{C})$	94.10	14.82	15.75 %

rea(G02N03620000901), and Regional Innovation Center (RIC) Program funded by the Ministry of Trade, Industry and Energy (MOTIE) and Korea Institute for Advancement of Technology (KIAT) through the Promoting Regional specialized Industry.

REFERENCES

- [1] H. Pan, Y. S. Hu, and L. Chen, *Emergy Environ. Sci.* 6, 2338 (2013).
- [2] L. Huang, J. Cheng, X. Li, and B. Wang, *J. Nanosci. Nanotechnol.*, 15, 6237 (2015).
- [3] B.C. Jang, S.B. Yang and J.T. Son, *J. Nanosci. Nanotechnol.*, 16 8352 (2016).
- [4] Y.J. Park, Y.S. Hong, X. Wu, K.S. Ryu, S.H. Chang, *J. Power Sources*, 129, 288 (2004).
- [5] X. Yang, X. Wang, L. Hu, G. Zou, S. Su, Y.S. Bai, H.B. Shu, Q. Wei, B.N. Hu, L. Ge, D. Wang, L. Liu, *J. Power Sources*, 242, 589 (2013).
- [6] Y.K. Sun, S.T. Myung, M.H. Kim, J. Prakash, K. Amine, *J. Am. Chem. Soc.*, 127, 13411 (2005).
- [7] B.C. Park, H.J. Bang, K. Amine, E. Jung, Y.K. Sun, *J. Power Sources*, 174, 658 (2007).
- [8] K.S. Lee, S.T. Myung, Y.K. Sun, *J. Power Sources*, 195, 6043 (2010).
- [9] H.J. Noh, S.J. Youn, C.S. Yoon, Y.K. Sun, *J. Power Sources*, 233, 121 (2013).
- [10] S.W. Cho, G.O. Kim, J.H. Ju, J.W. Oh, K.S. Ryu, *J. Materials Research Bulletin*, 47, 2830 (2012).
- [11] Y. Qi, Y. Huang, D. Jia, S.J. Bao, Z.P. Guo, *Electrochimica Acta*, 54, 472 (2009).
- [12] G.H. Kim, J.H. Kim, S.T. Myung, C.S. Yoon, Y.K. Sun, *J. Electrochem. Soc.*, 152, A1707 (2005).
- [13] C. Wu, F. Wu, L. Chen, X. Huang, *Solid State Ionics*, 152, 327 (2002).
- [14] M. Kageyama, D. Li, K. Kobayakawa, Y. Sato, Y.S. Lee, *J. Power Sources*, 157, 494 (2006).
- [15] S.H. Kang, K. Amine, *J. Power Sources*, 146, 654 (2005).
- [16] J.W. Mullin, *Crystallization Butterworths*, London, 1961.
- [17] G.W. Yoo, H.J. Jeon, J.T. Son *Journal of the Korean electrochemical Society*, 16, 59 (2013).
- [18] R.J. Gummow, M.M. Thackeray, W.I.F. David, *S. Hull Mater. Res. Bull.*, 27, 327 (1992).
- [19] S.U. Woo, B.C. Park, C.S. Yoon, S.T. Myung, J. Prakash, Y.K. Sun, *J. Electrochem. Soc.*, 154, A649 (2007).
- [20] G.G. Amatucci, N. Pereira, T. Zheng, J. -M. Tarascon, *J. Electrochem. Soc.*, 148, A17 (2001).
- [21] J.R. Dahn, U. von Sacken, C.A. Michal, *Solid State Ionics*, 44, 87 (1990).
- [22] J.N. Reimers, E. Rossn, C.D. Jones, J.R. Dahn, *Solid State Ionics*, 61, 335 (1993).